Electronic Supplementary Material (ESI) for Nanoscale.

Table S1 Pore-structure parameters of the pristine CAs with different densities.

sample	BET specific surface area ($m^2\ g^{-1}$)	Pore volume ($cm^3\ g^{-1}$)	Average pore diameter (nm)
CA (300 mg cm^{-3})	676.5	1.7	18.7
CA (170 mg cm^{-3})	738.5	2.9	27.7

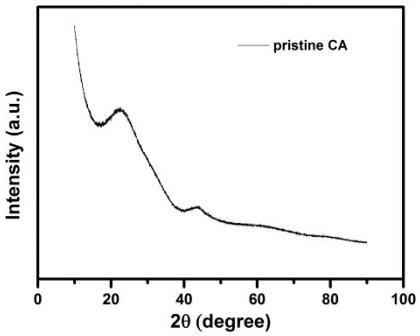

Fig. S1 XRD pattern of pristine CA.

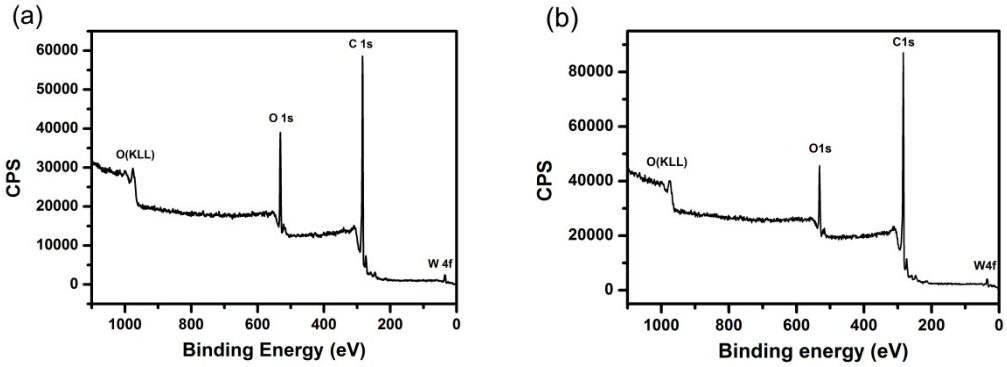

Fig. S2 XPS spectra: survey scan spectrum of (a) p-WO_3 and (b) pw-WO_3-C.

To find the real reason for the increase of C=O group, two experiments were conducted. On the one hand, the pristine CA was calcined under the same heat-treatment process without incorporating WO_3, and then XPS tests were conducted to examine the change of C1s peaks (shown in Fig. S3a). The results show that the content of C=O group do not change obviously. So it can be concluded that calcination of pristine CA in the air without incorporating WO_3 would not increase the content of C=O group apparently, although more defects may be generated.

On the other hand, for obtaining the more exact information of pw-WO_3-C, the absorbed air in the pores was excluded in a set of treatment processes. These processes briefly consisted of an outgassing process at N_2 atmosphere, a sample-transport process under N_2 atmosphere, and an ultra-long vacuum pumping process for over 39 h before the XPS examination. We considered that the influence of adsorbed air in the samples could be removed basically by such a set of treatment process. The results are showed in Fig. S3b and indicate that the content of C=O group is similar to the sample without air-exclusion treatment. Thus, the fact that the increase in the content of C=O group do not originate from the adsorptive CO_2 could be confirmed. Otherwise, it can also be concluded that the WO_3 incorporating would bring to an additional increase of C=O group. Consequently, we considered the increase of C=O group would result from the fact that

the carbon matrix is more likely to form the surface suspension bond with the assist of nano WO_3.

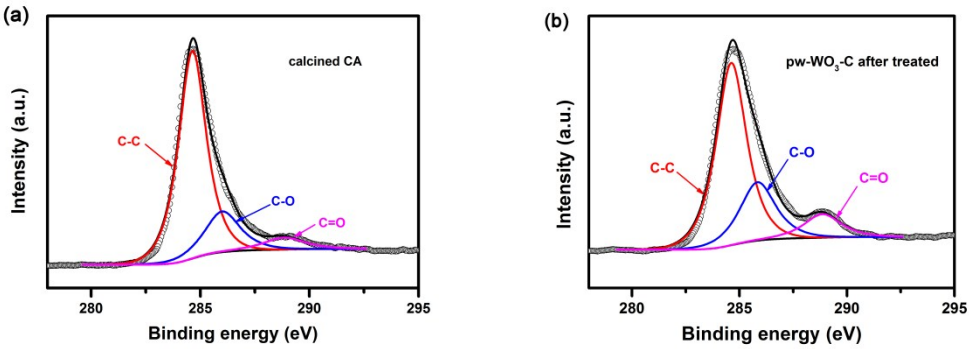

Fig. S3 The C 1s XPS spectra for (a) the calcined CA without WO_3 incorporating and (b) pw-WO_3-C after air-exclusion treatment.

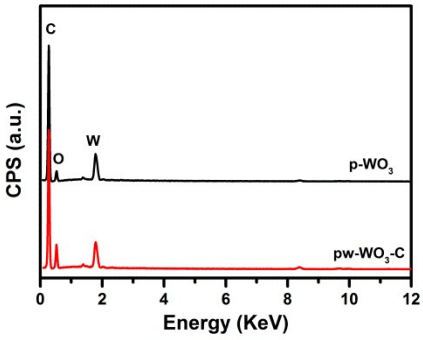

Fig. S4 EDS pattern of p-WO_3 and pw-WO_3-C.

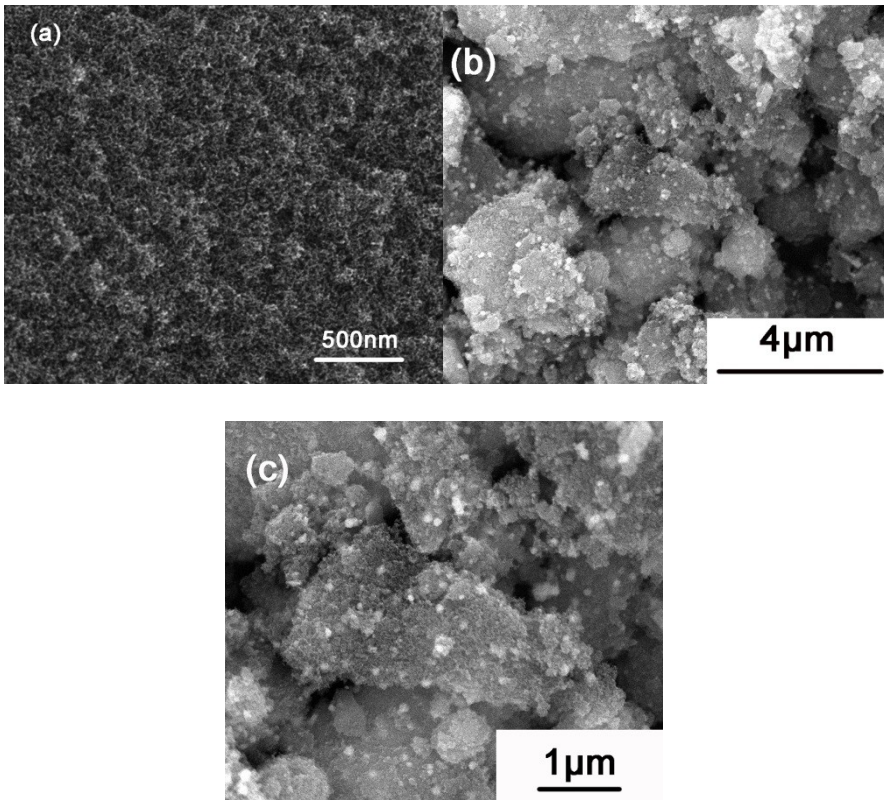

Fig. S5 SEM images of (a) pristine CA, (b) p-WO_3 under lower magnification and (c) p-WO_3 under higher magnification.

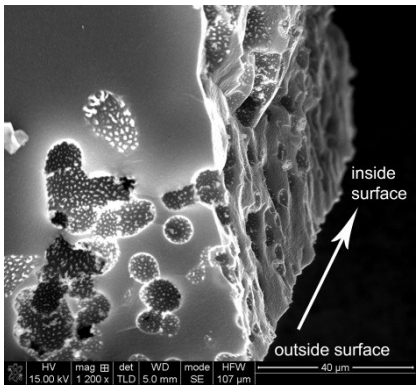

Fig. S6 Cross-sectional image of SEM for pw-WO_3-C.

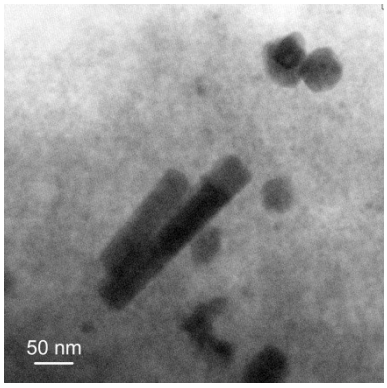

Fig. S7 TEM images of pw-WO_3-C after grinded.

In order to further prove the bonding of W, C and O, the selected area electron diffraction (SAED) and Raman tests were conducted. The SAED pattern was presented in Fig. S8. In the SAED pattern, we used white line and texts to annotate the WO_3 phase, and red ones to annotate the W_2(C,O) phase. We can find the interplanar distance of ~0.122 nm, which can correspond to (222) of W_2(C,O) phase. Meanwhile, the (111) and (311) planes of W_2(C,O) phase could also be distinguished. Thus, we considered that the SAED data could possibly support 'the bonding of W, C and O'.

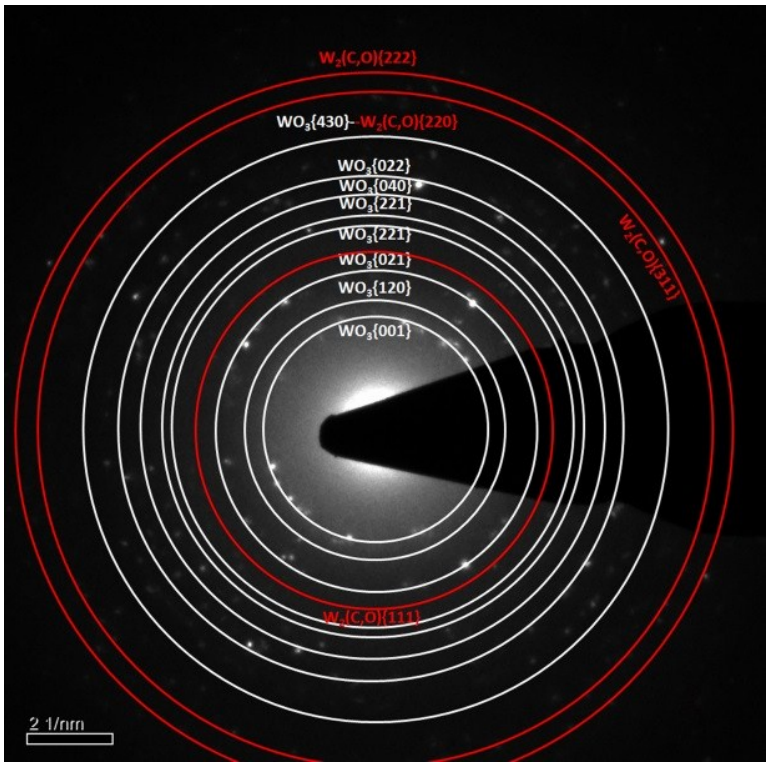

Fig. S8 SAED pattern of pw-WO_3-C.

Raman spectra of p-WO_3 and pw-WO_3-C were presented in Fig. S9. The characteristic peaks at the wavenumbers of 803 and 679 cm^{-1} are typical Raman peaks of the crystalline WO_3.[1, 2] The characteristic peaks at the wavenumbers of 803 and 679 cm^{-1} are typical Raman peaks of the crystalline WO_3.[1, 2] The peak at 803 cm^{-1} is assigned to stretching vibration of the bridging tungsten and oxygen atoms, while the peak at 679 cm^{-1} corresponds to the bending vibrations of W-O bonding. The peaks in the 200-400 cm^{-1} region can be assigned to O-W-O bending modes of binding oxygen.[3] It is also shown that pw-WO_3-C possesses the additional peaks (marked in the blue rectangle), compared to p-WO_3. The wide stage between 903 and 966 cm^{-1} may result from a superposition of the peaks at ~803 and ~960 cm^{-1}. The latter peak could be attributed to the stretching mode of W=O.[4] It is a pity that the peak at ~423 cm^{-1} can not be well indexed, due to a lack of the related reported literature. However, regarding this peak at ~423 cm^{-1}, we can offer some possible evidences, according to the reported data of Raman tests. For such low wavenumber, this peak probably results from the bond containing W. The pw-WO_3-C contains only the C, O and W elements and both the W-C bond and W-O band can not be assigned to the peak at ~423 cm^{-1}.[1-5] Therefore, the bonding of W, C and O can possibly be taken into account. In addition, we can find the similar peak shown in the reference 5. The specific descriptions about this peak can not be achieved from this reference, but it can be deduced that this peak may result from the 'incipient oxidation of the WC phases' based on the similar analysis in this reference. Thus, synthetically considering the above evidences, we believed that this peak centered at ~423 cm^{-1} from Raman spectra could possibly be attributed to the bonding of W, C and O.

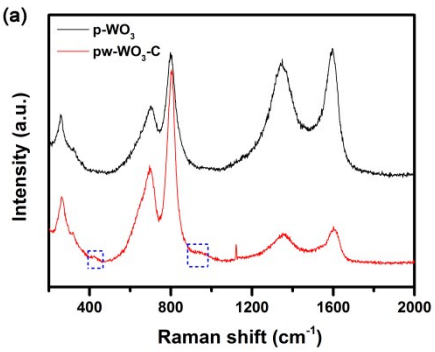

Fig. S9 Raman spectra of p-WO_3 and pw-WO_3-C.

To confirm the valence transformation of the two reversible peaks (1/1' and 2/2'), the ex-situ XRD and ex-situ XPS tests have been conducted. The electrodes of pw-WO_3-C were discharged in 2M H_2SO_4 to different voltage (-0.1 V and -0.3 V *vs.* Ag/AgCl) and then the electrodes were dried at 80 ^oC for 3 days.

Fig. S10 shows the XRD spectra of the electrode of pw-WO_3-C under different discharging conditions. The strength of diffraction peaks changes with the electrode discharge. The strength of (221) planes increases and the strongest peaks seem to become a little wider, accompanied by the protons insertion into the crystal structure. Note that the orthorhombic phase of WO_3 maintains in the discharge process and no new phase can be observed.

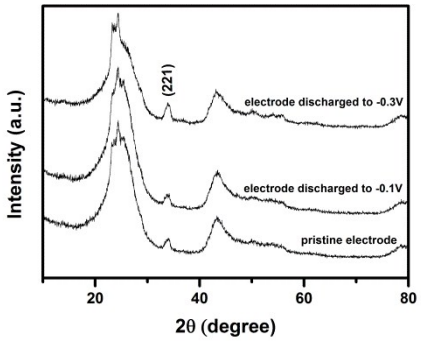

Fig. S10 XRD patterns for pristine electrode and the electrode discharged to -0.1V and -0.3V of pw-WO_3-C.

Fig. S11 shows the XPS spectra of the electrode of pw-WO_3-C under different discharging conditions. It is shown that the binding energies have shifted with the addition of the binder (PVDF) in the process of electrode preparation. Except for the main peaks of W^{6+}, the peaks of tungsten oxide in lower valence state could also be observed for both the discharging samples. With respect to the peak position, there are little differences between the sample discharged to -0.1 V and the one discharged to -0.3 V. Based on the measurement results, we considered that the two reversible peaks mean the mutual transformation of tungsten oxide between higher valence state and lower valence state, but the specific transformation process can not be distinguished.

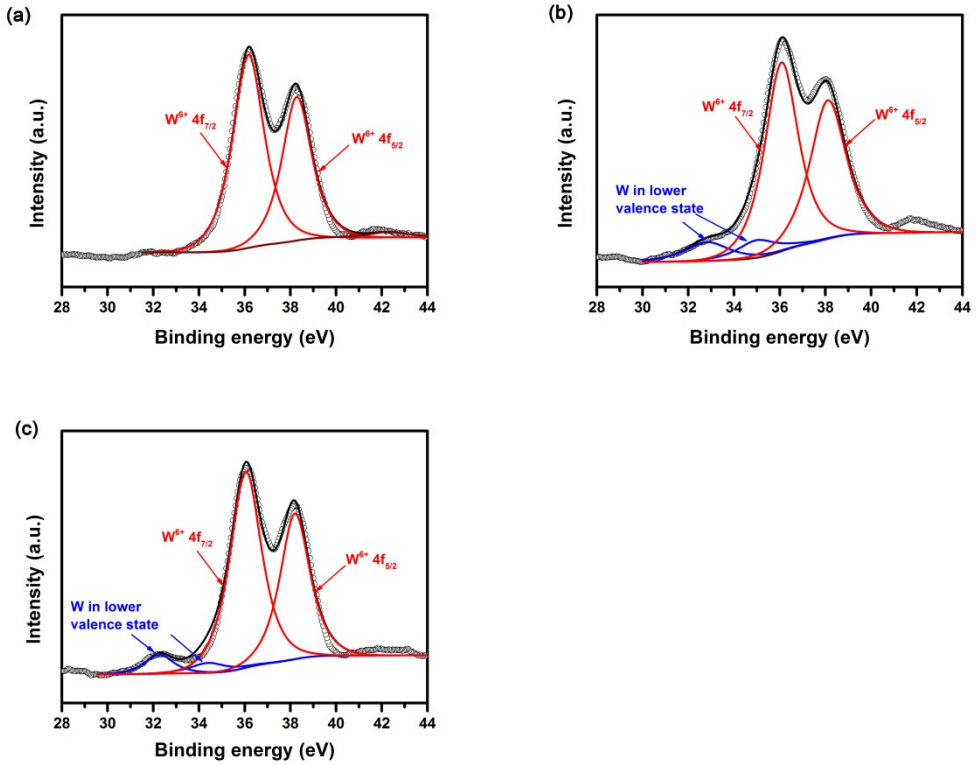

Fig. S11 The W 4f XPS spectra for (a) pristine electrode and the electrode discharged to (b) -0.1V and (c) -0.3V of pw-WO_3-C.

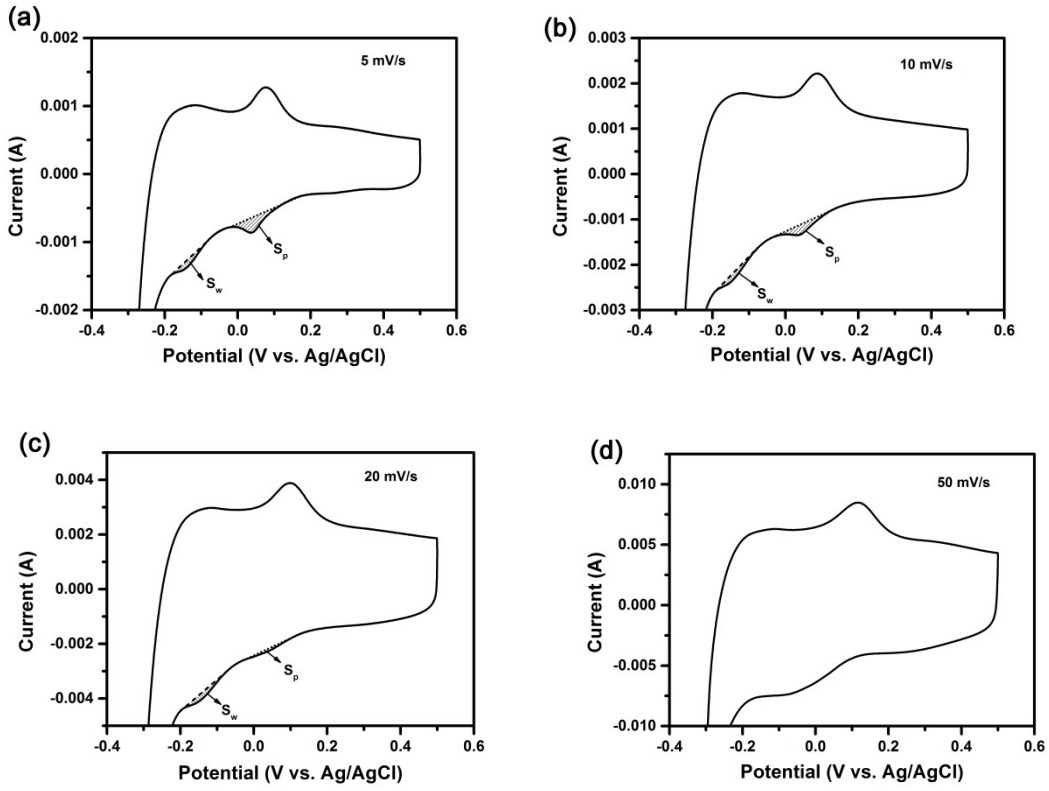

Fig. S12 Illustration of peak area for WO_3 nanowires and nanoparticles at (a) 5 mV s^{-1}, (b) 10 mV

s^{-1}, (c) 20 mV s^{-1} and (d) 50 mV s^{-1}.

References

1 S. Rajagopal, D. Nataraj, D. Mangalaraj, Y. Djaoued, J. Robichaud and O. Y. Khyzhun, *Nanoscale Res. Lett.*,2009, **4** ,1335-1342.

2 Y. Cai, Y. D. Wang, S. J. Deng, G. Chen, Q. Li, B.Q. Han, R. Han and Y. D. Wang, *Ceram. Int.*, 2014, **40**, 4109-4116.

3 Y. Baek and K. Yong, *J. Phys. Chem. C*, 2007, **111**, 1213-1218.

4 J. C. Sánchez-López, D. Martínez-Martínez, M. D. Abad and A. Fernández, *Surf. Coat. Tech.*, 2009, **204**, 947-954

5 S. E. Mrabet, M. D. Abad, C. López-Cartes, D. Martínez-Martínez and J. C. Sánchez-López, *Plasma Process. Polym.*, 2009, **6**, S444-S449.